Projections of future fire risk under climate change over the South African savanna

Mukovhe V. Singo[1,*], Hector Chikoore[2], Francois A. Engelbrecht[3], Thando Ndarana[4], Tshimbiluni P. Muofhe[3], Innocent L. Mbokodo[5], Florence M. Murungweni[1], Mary-Jane M. Bopape[6]

[1] Department of Geography and Environmental Sciences, University of Venda, Thohoyandou, South Africa

[2] Department of Geography and Environmental Studies, University of Limpopo, Sovenga, South Africa

[3] Global Change Institute, University of the Witwatersrand, Johannesburg, South Africa

[4] Department of Geography, Geoinformatics and Meteorology, University of Pretoria, Hatfield, South Africa

[5] Climate Services, South African Weather Service, Centurion, South Africa

[6] South African Environmental Observation Network, National Research Foundation, Pretoria, South Africa

*Correspondence to Mukovhe V. Singo. Email: singomv9@gmail.com

Abstract

Rising surface air temperatures, coupled with delays in the onset of austral summer rains and increased fuel load have amplified forest fire risk over southern Africa. This study investigates interactions between climate change and fire risk in South Africa's northern savanna biome. We employ the CCAM model to simulate the reference climate and project future forest fire risk on the savanna. An ensemble of six CMIP5 GCMs were downscaled to 8 km to project climate change in the far-future (2080 to 2099) under RCP8.5 emission scenario. The models were validated using ERA5-Land reanalyses whilst future projections focused on the 10th, 50th and 90th percentiles. The frequency of high fire risk days was calculated using a McArthur Forest Fire Danger Index (FFDI) which links meteorological variables to fire danger. The ensemble simulated widespread temperature rises of between 4.5 and 6 °C across the savanna, whilst rainfall is projected to decline by up to 20 mm/month, with corresponding decreases in minimum relative humidity. Heat wave days are projected to increase to above 8 days per annum, whilst soil moisture deficiency increases by above 50 mm on the savanna. Consequently, mean annual high fire danger days are projected to reach a peak frequency of 25 days in October, with an autumnal secondary peak. Spatially, greater increases in high FFDI days were projected over the western savanna extending toward neighbouring Botswana. This study contributes to understanding fire risk under unprecedented temperature rises which appear to be modulating fire intensity in the study region.

Keywords: Climate change; Fire risk; Fire regimes; Keetch-Byram Drought Index; McArthur Forest Fire Danger Index; Savanna

1 Introduction

Fire plays a significant role in the earth system, and regardless that some terrestrial ecosystems are fire sensitive, wildfires are not foreign ecological disturbances (Bowman et al. 2020; Cochrane et al. 2021). Sub-tropical and tropical ecosystems require frequent fire to curb woody plant encroachment since fire is important for the structure, composition, and dynamics of areas (Gordijn et al. 2018). Savanna fires occur frequently, mostly in tropical regions (Flannigan et al. 2009). African savannas are fire prone ecosystems, with most wildfires occurring during the dry season (Laris et al. 2020). In most of subtropical Africa, the dry season lasts for half of the year due to the migration of the tropical rain belts. The distinct dry and wet seasonality in Africa directly affects fuel moisture, fuel load and fire intensity, which vary from season to season (Platt et al. 2015). Besides, wildfire occurrence and behaviour have been evolving during recent decades in several regions worldwide, becoming more severe and more frequent (Keeley and Syphard 2021).

Whilst landscape fires may even have some positive effect on some vegetation species, wildfires are often intense and with devastating impacts (United Nations Environment Programme 2022). Wildfires occur in ecosystems as a function of climate, human activities, and vegetation types (Cochrane et al. 2021). Humans have altered factors that shape fire regimes by changing timing of ignitions, climate and fuels (Archibald 2016; Rogers et al. 2020). Other factors that shape fire regimes include fire frequency, severity, intensity, type, seasonality and spatial scale (Cochrane et al. 2021). By far, most wildfires are ignited by human interactions with landscapes which influence flammability (Viedma et al. 2018). Thus, impacts of human factors on wildfires override the role which climate plays and their varying nature makes them complex (Viedma et al. 2018). Variations caused by human factors involve decreasing fires through enforcing suppression policy or increasing fire activities due to Land Use/Land Cover changes (Bajocco et al. 2019; Schmidt and Eloy 2020).

A large proportion of burned areas and biomass emissions around the globe are identified in African savannas (Platt et al. 2015). Biomass burning is a significant source of atmospheric pollutants (gasses and particulates) at regional and global scales (Crutzen et al. 1979). Atmospheric gases such as carbon monoxide (CO), carbon dioxide (CO_2), methane (CH_4), volatile and semi-volatile organic compounds, aldehyde, organic acid and inorganic elements and particulate matter (PM) are released during burning of biomass materials (Yadav and Devi 2019). The continuous emission of CO_2 into the atmosphere stimulates growth of vegetation biomass (Hovenden et al. 2019). Emissions and increases of CO_2 in the atmosphere are caused by fossil fuel burning, and the elevated levels of CO_2 stimulate growth in some vegetation species (Lobo et al. 2022).

Climate is one of the contributing factors that define fire regimes with the interaction of topography and available fuels (Countryman 1972; Kasischke and Hoy 2012). Most large fires that occur worldwide are influenced (ignition and propagation) by prevailing weather conditions (Duane and Brotons 2018), hence directly affecting vegetation moisture content and fire behaviour, which becomes extreme under high temperatures, low humidity and windy conditions (Piñol et al. 1998). Land use change and associated climate related stress factors induced extreme events such as droughts and heatwaves which influence the occurrence of wildfires (Roces-Diaz et al. 2021). Accumulated dead biomass and other fine flammable fuels are vulnerable to ignite under strong winds while inducing high intensity fires (de Groot et al. 2010).

The southern Africa region is largely a semi-arid region with strong warming induced by the descending branches of the Hadley cell (Mahlobo et al. 2019). The main rainy season occurs during the austral summer months from October to April influenced by tropical-extratropical cloud bands or tropical-temperate troughs (TTTs) that contribute nearly half of the regional summer rainfall (Harrison 1984; Hart et al. 2010, 2013). The main synoptic weather system that affects fire regimes over the southern Africa region is the subtropical high-pressure belt which is divided by the continent yielding a continental high, the South Atlantic Ocean High and the Indian Ocean High (Tyson and Preston-Whyte 2000; Dyson and van Heerden 2002). Subsiding air suppresses precipitation, sunny and clear skies prevail enhancing drying of fuels during winter season over southern Africa (van der Walt and Fitchett 2020). The austral winter season over South Africa corresponds with the dry season over much of the subcontinent and the airflow is predominantly dry, anticyclonic, and subsiding (Tyson and Preston-Whyte 2000). Strong drainage foehn-type winds locally known as berg (mountain) winds are associated with most large fires and heat waves that occur near the coasts in South Africa. This occurs ahead of a cold front, when air from the continental high over the interior plateau descends a 1000 m high escarpment towards a coastal low, warming adiabatically in the process (Tyson and Preston-Whyte 2000).

Typically, intense dry spells occur when a mid-tropospheric anticyclone (Botswana High) develops over Namibia/Botswana coupled with ocean warming east of Madagascar drives atmospheric moisture away from the continental interior (Chikoore and Jury 2021). The Botswana High is found to have strong positive correlation with dry spell (drought) frequencies and extreme temperature days during summer over southern Africa (Driver and Reason 2017). Extreme drought conditions occur over southern Africa under strong Pacific El Niño conditions, a strengthened westerly jet stream and a positive Indian Ocean Dipole mode (Chikoore and Jury 2021). Dry and hot conditions create conditions suitable for drying of the fuel load and forest fire ignition through spontaneous combustion. Several other studies have considered the significant role of weather and climate variables on wildfire activity (e.g., Engelbrecht et al. 2015; Keeley et al. 2016; Kraaij et al. 2018).

Climate change disturbances to ecosystems are expected to intensify in future with catastrophic events such as prolonged droughts affecting the tropical savannas (Sankaram 2019). Furthermore, the tropical savanna climate is projected to become more vulnerable to extreme heatwaves, high fire frequencies, and loss of vegetation cover (Hoffmann et al. 2002). The onset of the summer rainy season is projected to delay considerably by 2070–2099 across southern Africa (Wainwright et al. 2021; Engelbrecht et al. 2015), through considerable drying in the austral spring. As the climate gets warmer, precipitation becomes more intense but less frequent which affects health of ecosystems. Rainfall intensity directly affects soil water availability from the surface to the deeper soils. An increase in rainfall amounts enhance deep soil water availability which in turn supports rapid growth of woody plants that have deep roots systems resulting in bush encroachment in savanna ecosystems (Engelbrecht and Engelbrecht 2016; Berry and Kulmatiski 2017).

The Köppen-Geiger climate zones are also projected to change when global temperatures increase by up to 3 °C (Engelbrecht and Engelbrecht 2016). High-resolution regional climate models showed south-westwards expansion of tropical savanna zone to South African east coast and invasion of woody cover into grasslands (Engelbrecht and Engelbrecht 2016). In addition, the semi-arid region is observed to have shifted hundreds of kilometres eastwards across South Africa (Jury 2021). There are also large uncertainties in future projections of vegetation biomes across Africa due to climate and CO_2 changes. Improved high resolution

model simulations of these impacts may provide highly flexible strategies for climate change adaptation (Martens 2020).

Climate change induced unprecedented increases in surface air temperatures over southern Africa due to heavy use of fossil fuels as the main source of energy, associated with high carbon emissions. By the end of this century (2100), global warming levels are projected to have increased by up to 4 °C in this region under the SSP5-8.5 worst-case emission scenario (Engelbrecht and Monteiro 2021). Global Climate Model (GCM) projections under the 1.5 °C global warming level have projected South Africa becoming warmer and drier in the middle of the near future term from 2021 to 2040 (Engelbrecht and Monteiro 2021).

It is against this background that this study uses high-resolution climate simulations for the Limpopo province, South Africa to asses future climate change and future changes in fire risk in the study region. The paper is divided as follows: the data and methods are presented next; Sect. 3 presents baseline climatologies of key fire weather variables and indices, whilst future climate change projections are detailed in Sect. 4; a synthesis of key findings and conclusion are provided at the end.

2 Data and methods

2.1 Study area

This study focuses on the north-eastern region of South Africa, a largely semi-arid region that shares its boundaries with Zimbabwe (north), Botswana (west), and Mozambique in the east (Fig. 1). The savanna biome, but with patches of grassland, forest and alluvial fans distinctively occupies the area (Val et al. 2021; Moshobane et al. 2021). The study area includes the renowned Kruger National Park on the eastern boundary, one of South Africa's largest wildlife reserves. Due to the aerial extent of the study region downscaling was necessary to obtain high resolution simulations of climate change projections and the future climate impacts on fire risk in the study area.

The Limpopo savanna is located in a semi-arid region associated with high temperatures significantly influenced by its location in the subtropics where the subtropical highs are dominant. Once established, the mid-tropospheric Botswana High induces summer drought and high temperatures or heat waves over southern Africa (Chikoore and Jury 2021). Drought events are often accompanied by extreme heat waves over the region (Lyon 2009, Chikoore and Jury 2021, Nembilwi et al. 2021) establishing compound extremes which often increase forest fire risk. Extreme maximum temperatures are influenced by climate change, through mid-level high pressure systems that subside as part of the Hadley cell cause high frequency heatwaves (Engelbrecht et al. 2015).

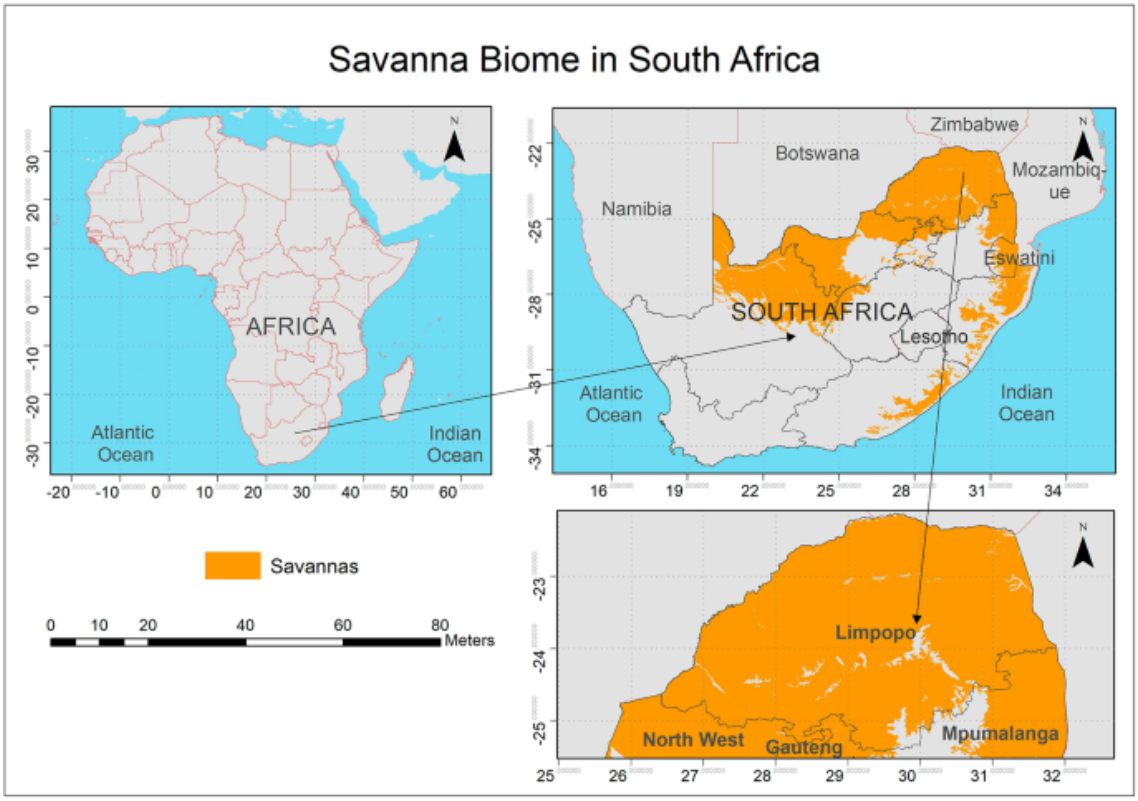

Fig. 1. The geographical location of South Africa on the African continent and the distribution of the savanna biome. This study focuses on the northern savanna (shown in orange) dominating the Limpopo Province. 2.2. Observation data

We employ the state-of-the art ERA5-Land reanalysis datasets (Muñoz Sabater et al. 2021) as the 'observed' data, which are available from the ECMWF at monthly temporal resolution. Essentially, the ERA5-Land reanalysis is gridded at a spatial resolution of 0.1° x 0.1° equivalent to 9 km using a reduced Gaussian grid (TCo1279) (Muñoz Sabater et al. 2021). Whilst the ERA5-Land data are available from 1950 to present, the designated period for the reference climate in this study is from 1961 to 1980. Surface air temperature (t2m) was the main observed variable which was used to analyse long term trends from 1961 to 2020. Temperature was also to investigate models' performance used in the study.

2.2 Coupled models

This study employed six (6) GCMs (see Table 1.) from the CMIP5 suite computed under the RCP8.5 (this representative concentration pathway represents the business-as-usual emission scenario). Dynamical downscaling of the six GCMs was performed by means of a regional climate model (RCM) (i.e., the Conformal-Cubic Atmospheric Model (CCAM)) to obtain a comparatively high spatial resolution of 8 km over the study area. The CCAM, originally developed at Australia's Commonwealth Scientific and Industrial Research Organisation (CSIRO), is based on a variable-resolution conformal-cubic grid to simulate regional scales barring lateral boundary conditions (McGregor 2005; Thatcher et al. 2015). It is among the first "cube-based three-dimensional" (3-D) atmospheric models avoiding lateral boundary stipulations and allows coupling together with the "global and regional spatial scales" on an

equal grid (Thevakaran et al. 2015). The model uses a non-hydrostatic, semi-implicit, and semi-Lagrangian dynamical core that is cost-effective for regional climate modelling due to semi-Lagrangian methods that allow longevity of time-step (McGregor 2005). It also has a sizable sequence of physical parameterizations to calibrate forces and energy transformation to describe the behaviour of the radiation, convection, aerosols, cloud microphysics, boundary layer turbulence, gravity wave drag, and land surface (Thevakaran et al. 2015).

Table 1. Six CMIP5 downscaled Global Climate Models

Models	Resolution	Institution	Source
Australian Community Climate and Earth System Simulator Coupled Model (ACCESS-CM)	Horizontal scale of 1–2 Km	Commonwealth Scientific and Industrial Research Organisation	Bi et al. (2013)
The Community Climate System Model (CCSM) version 4	Atmosphere and land resolution of 1°	National Center for Atmospheric Research	Gent et al. (2010)
Centre National de Recherches Meteorologiques Climate Model (CNRM-CM) version 5.1	Horizontal 1.4° and Ocean 1°	Centre National de Recherches Meteorologiques-Groupe d'etudes de l'Atmosphere Meteorologique	Voldoire et al. (2013)
Geophysical Fluid Dynamics Laboratory Earth System Models (GFDL-ESM) version 4.1	Horizontal 2° to 1° and ocean 1° to 0.5°	Geophysical Fluid Dynamics Laboratory	Dunne et al. (2020)
Max Planck Institute Earth System Model (MPI-ESM) version 1.2	Horizontal resolution T127 (~100 km) and Ocean 0.4°	Max Planck Institute	Müller et al. (2018)
Norwegian Earth System Model (NorESM) version 2	Horizontal 2°	University Corporation for Atmospheric Research	Seland et al. (2020)

In addition to 2 m maximum temperature (tmax), the ensemble of six models simulates precipitation (rnd24), 10 m wind (u10), minimum relative humidity (rhmin), heatwave days, Keetch-Bryam Drought Index (KBDI). The variable "heatwave days" refers to the number of days under heatwave conditions in a certain area. While it is acknowledged that several definitions of heatwaves exist in the refereed literature, heatwaves are defined as the period of at least three consecutive days whereby an average maximum temperature of the warmest month is exceeded by a threshold of 5 °C at a specific location over the study area (Mbokodo et al. 2020).

The KBDI index (Keetch and Bryam 1968) is an index widely used in evaluating the conditions conducive for wildfire activity (Gannon and Steinberg 2021). was employed to simulate soil moisture deficiency over the savannas. The KBDI index is a measure of soil moisture deficiencies in the topsoil and has been used in forest fire risk assessment (NIDIS 2022). The KBDI is derived from ground-based estimates of precipitation and temperature and hence evapotranspiration to estimate surface soil moisture deficits (Gannon and Steinberg 2021). In millimetres, the index ranges from 0 to 200, with 200 being the worst drought (extremely dry) possible and 0 indicating no soil moisture deficiency (NIDIS 2022). Essentially the higher the KBDI value, the higher the risk of forest fire.

To determine the impact of rising surface air temperatures on fire risk on the South African savannas, we employed the McCarthy Forest Fire Danger Index (FFDI) to calculate the number of days per annum with high fire danger. The FFDI is calculated using air temperature, relative humidity, surface winds and a drought factor which represents fuel availability (Noble et al. 1980; Dowdy 2018). The KBDI defined above is incorporated into the FFDI as the drought factor and therefore the indicator for surface soil moisture deficiency. As the FFDI is directly proportional to the KBDI, the higher the FFDI value, the higher the potential risk for a bush fire.

2.3 Model statistical validation and climate change projections

A Taylor diagram (Taylor 2001), a two-dimensional (2-D) graph that summarizes the strength of the relationship between a set of models and observations was used to evaluate models' performance in simulating the historical baseline (1961–1980) climatologies in the present study. The Taylor diagram comprises the centered Root Mean Square Error (RMSE), a correlation coefficient (r), and a normalised standard deviation plotted simultaneously on a single quadrant (Taylor 2005). The values of surface mean air temperatures were plotted with normalized variance to show the relative amplitude of the models and observed variations (Hu et al. 2019).

Future climate projections were derived from an ensemble of six CMIP5 GCMs that were experimented under the RCP8.5 worst-case emission scenario and dynamically downscaled by the regional climate model CCAM into a very high resolution of 8 km. Model simulations were analysed separately and also as ensembles for the variables mentioned above for the reference period (1961–1980), the near future (2021–2040), mid future (2041–2060), and far future (2080–2099). However, we focus mainly on anomalies in the far-future where we subtract the reference climatology from the projected future climate. We selected the 10th, 50th and 90th percentiles to analyse spatial variability of rainfall, maximum temperature, minimum relative humidity, heatwave days, wind speed, KBDI index and high fire danger days. Percentiles are often used in climate change projections to indicate the spread of uncertainty associated with the future projections for each variable. They can be defined as values on a scale of one to hundred below which certain proportions of observations fall (Bornmann et al. 2013).

3 Results and discussion

3.1 Reference climate

3.1.1 Observed and simulated temperature trends

We analysed the mean surface (2 m) air temperatures for the reference climate and mean for the two most recent decades (2001–2020) indicating increasing temperatures across the entire study area. Globally, 19 of the warmest temperatures have occurred during this later period (2001–2020), with 2016 as the hottest, coinciding with the strongest El Niño event on record (NASA 2022). The changes in surface air temperatures that have occurred between the two 20-year periods (2001–2020 and 1961–1980; Fig. 2) show widespread warming with a range between 0.4 and 0.5 °C along longitude ~ 31°E which coincides with high topography called the Great Escarpment (Fig. 2c). Elsewhere, higher changes of 0.6 to 0.7 °C can be observed across the study area including the lowlands in the north, west and east. Even dangerous temperature rises (from 0.8 °C to above 1 °C) have occurred over the Highveld in the south, which may be linked to intensification of the Hadley Cell (e.g., Mahlobo et al. 2019). In addition to present day temperature trends, the historical reference (1961–1980) climatologies of air temperatures of six GCMs from the Coupled Model Intercomparison Project Phase 5 (CMIP5) are analyzed (Fig. 3). A visual inspection of spatial patterns of surface air temperatures simulated by GCMs closely resembles the ERA5-Land reanalysis in Fig. 2a. A more robust statistical verification of the same is presented in Sect. 3.1.2.

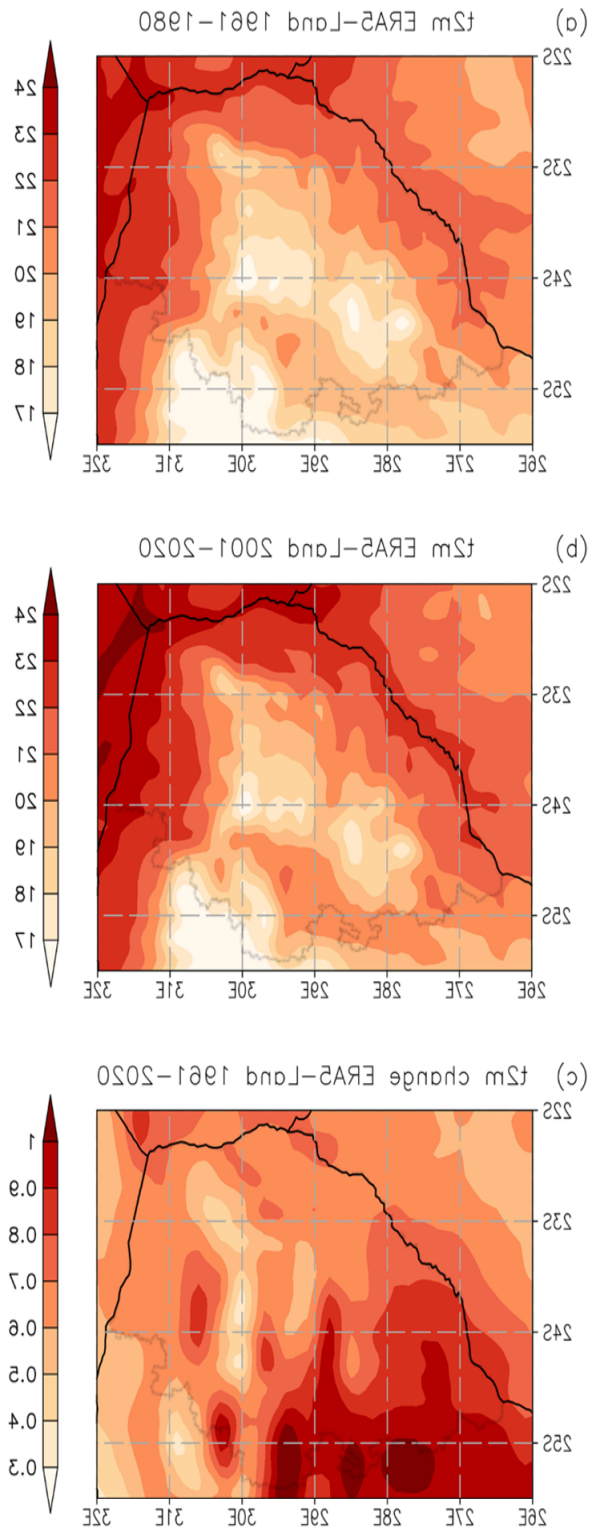

Fig. 2. ERA5-Land reference climate average surface air temperature at 2 m (t2m) (°C) observations for the periods (a) 1961–1980; (b) 2001–2020; and (c) the change over time. Darker shades represent higher surface air temperature (a, b) and higher temperature changes in (c)

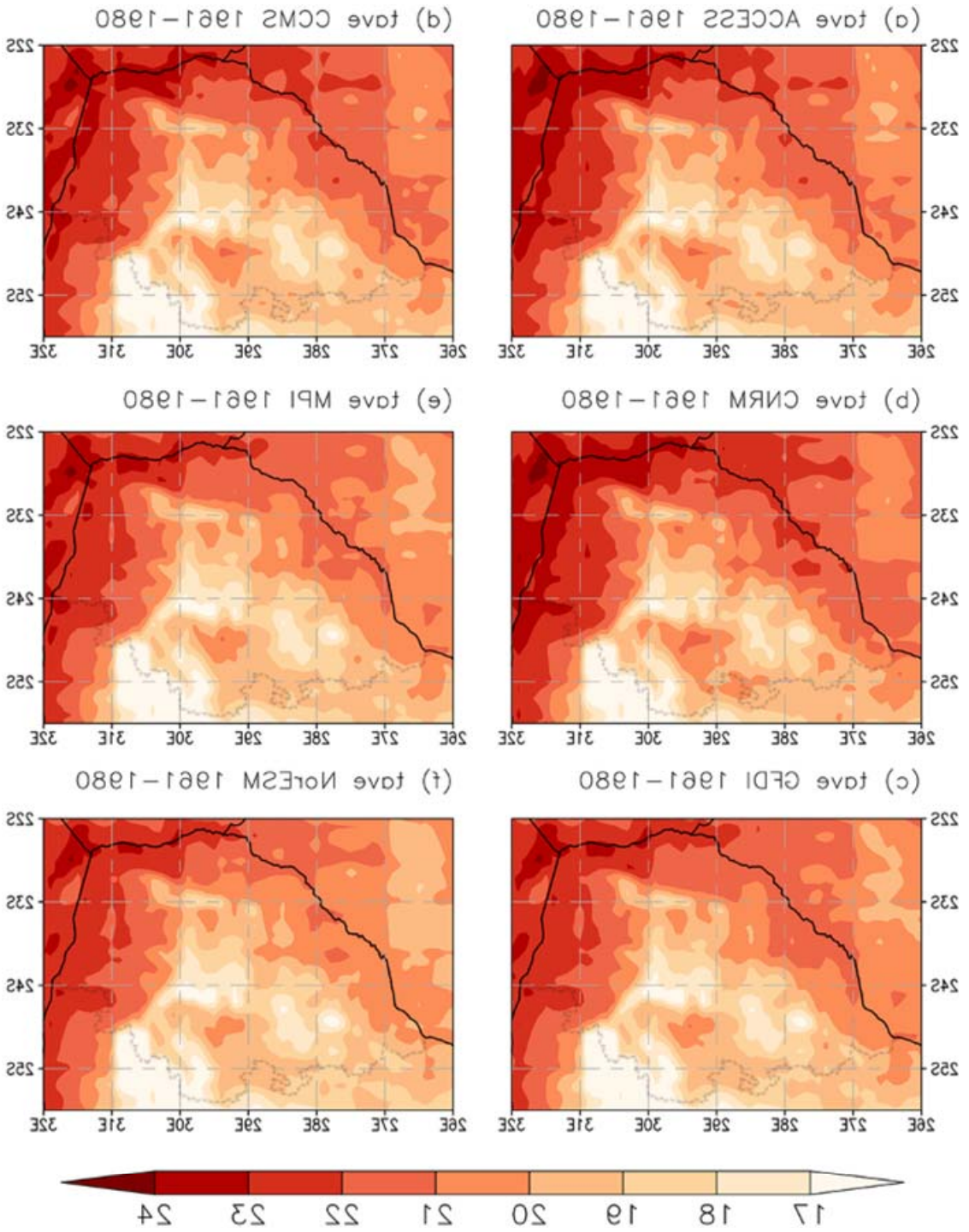

Fig. 3. Simulations of average 2 m air temperature (°C) from six CMIP5 models for the historic baseline period 1961–1980. Darker shades represent higher surface air temperature

3.1.2 Models' statistical verification

The models' statistical validation demonstrated high performance from all 6 model downscalings in comparison with the ERA5-Land surface (2 m) air temperatures. The NorESM slightly overestimated temperature variability, whilst models CCSM, CNRM-CM, and GFDL-

ESM showed very close variability to observation. Meanwhile, the GFDL-ESM was the least performing model in terms of correlation and RMSE. The models performed very well in terms of all statistics employed in the Taylor diagram with high correlation coefficient above 0.97, least RMSE around 0.2 and below and close variability in terms of the normalised standard deviation (Fig. 4).

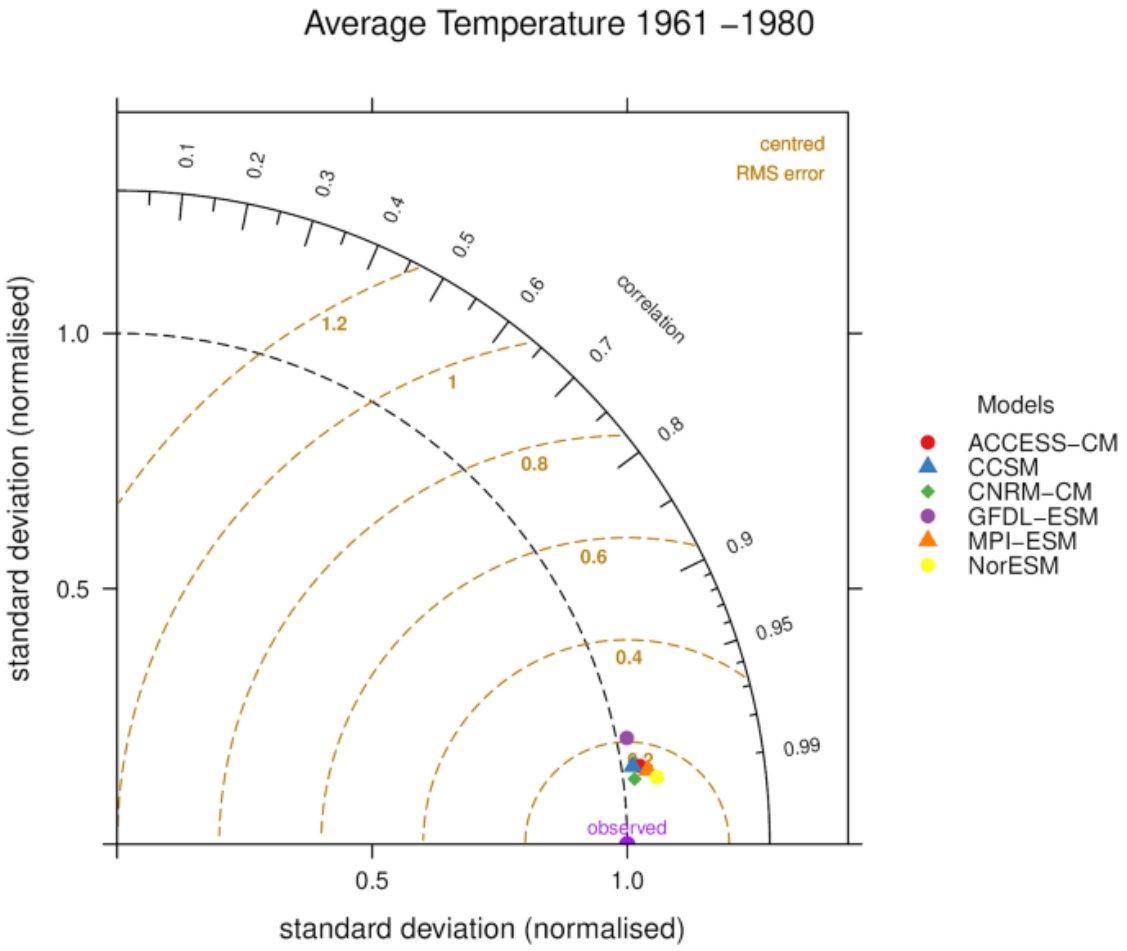

Fig. 4. Taylor diagram showing the performance statistics of the six CMIP models against the ERA5 reanalysis (observed) for 2 m surface air temperatures

3.1.3 GCM simulations

The simulated baseline climatologies for the period 1961–1980 are shown in Fig. 5 based on the 50th percentile of an ensemble of six regional simulations downscaled from the CMIP5 GCMs. An analysis of spatial and temporal variability of rainfall, minimum relative humidity, maximum temperature, wind speed, soil moisture deficiency and heatwave days (Fig. 5a-f) is critical in understanding wildfire risk over the Limpopo savanna.

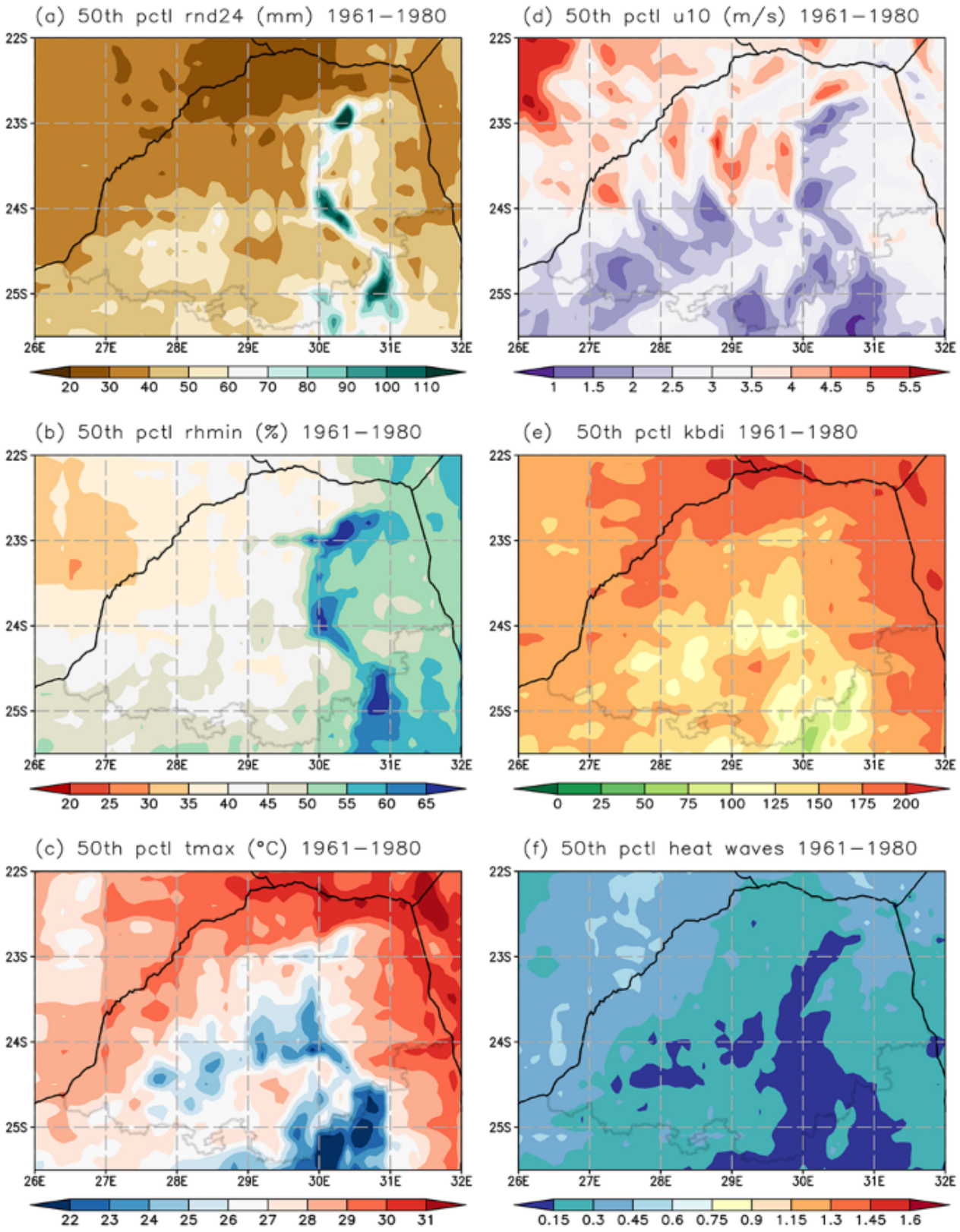

Fig. 5. Baseline climatologies (1961–1980) for the CMIP5 ensemble based on the 50th percentile annual average for (a) rainfall; (b) minimum relative humidity (%); (c) maximum temperature (°C); (d) windspeed at 10 m; (e) Keetch–Byram drought index (mm); and (f) heatwave days

The study area is considered a semi-arid region, where rainfall is spatially highly variable across the study area with more rainfall occurring along north-eastern Great Escarpment (~ 30°E-31°E longitude) enhanced by orographic effects to amounts well above 110 mm/month in places (Fig. 5a). Whilst the Limpopo savanna is largely semi-arid, some of the highest rainfalls (~ 1800 mm/yr) in South Africa are found on the mountain ranges in this region (Chikoore et al. 2021). The very high rainfall here supports large-scale commercial agriculture including eucalyptus and sugarcane plantations (Maponya et al. 2021). The rest of the region receives mean rainfall of 40 to 70 mm/month in the south, with drier conditions in the border areas below 40 mm/month (Fig. 5a). The drier region (22–23°S) near the borders between Botswana, Zimbabwe and South Africa forms part of the Limpopo River Valley. In this region, a 'drought corridor' was identified from 20–25°S characterized by frequent dry spells (Usman and Reason 2004).

The minimum relative humidity field shows similar spatial variability patterns to rainfall, resembling moist conditions with minimum relative humidity of 65% along the ~ 30°E longitude and Great Escarpment (Fig. 5b). Whilst the minimum relative humidity showed a gradual decrease to the east, it is far drier in the west towards Botswana. The eastern region is more humid as moisture in Limpopo is largely imported from the western Indian Ocean in the east (Rapolaki et al. 2020, Ndarana et al. 2022). The drier lowlands near the boundaries are also warmer, with high maximum temperatures ranging between 28 and 31 °C (Fig. 5c). The mean maximum temperatures on the interior and the Highveld in the south range from 22 to 28 °C.

Wind speed is the most complex meteorological variable, considering the wind gusts and local winds that are due to topography or thermally induced circulations. Mean 10 m wind speeds during the reference climate are generally between 1 m/s to 3 m/s over much of the savanna (Fig. 5d). However, for the region between 22–23°S, from Botswana, along north regions of the study area to Zimbabwe and Mozambique, higher mean wind speeds were simulated high wind speeds ranging between 3.5 m/s and 5 m/s. These higher speeds may also be related to the presence of a nocturnal low-level jet stream, locally known as the Limpopo Jet, responsible for transporting water vapour over Limpopo River valley (Barimalala et al. 2021; Munday et al. 2021; Spavins-Hicks et al. 2021).

The reference climate of the KBDI simulated dry conditions, mostly in the border areas with Mozambique, Zimbabwe and Botswana, which includes the Lowveld and the Limpopo River Valley (Fig. 5e). In the central and south regions, soil moisture availability remains high because of low evaporation proving lower fire risk over the regions. Simulated average heatwaves days are relatively low over the Limpopo savanna in the historical baseline (Fig. 5f).

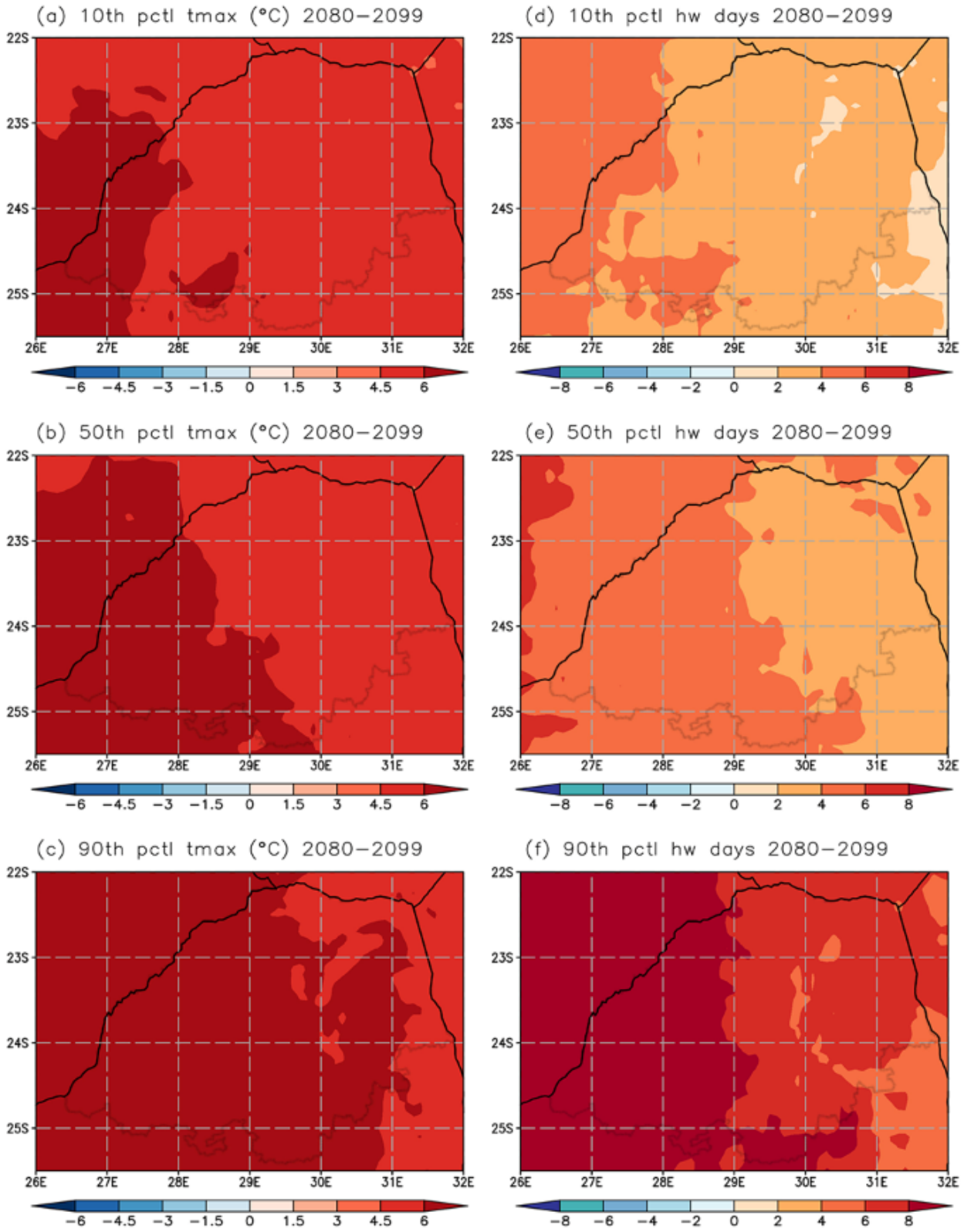

Fig. 6. Far future (2080–2099) projected changes in (a) 10th percentile maximum temperature (°C); (b) 50th percentile maximum temperature (°C); (c) 90th percentile maximum temperature (°C); (d) 10th percentile heatwaves days; (e) 50th percentile heatwaves days; and (f) 90th percentile heatwaves days. Darker shades of red indicate greater positive anomalies in tmax values and heatwave days

3.2 Projections of far future climate change and fire regimes over the Limpopo savanna

3.2.1 Projected changes in maximum temperatures and heatwaves

Projected changes in maximum temperatures and heatwave days using the 10th, 50th and 90th percentiles are shown in Fig. 6. Maximum temperatures in the far future are projected to increase drastically to range from + 4.5 °C to + 6 °C across the Limpopo savanna (Fig. 6a-c) in relation to the reference period 1961–1980. Under the 10th percentile, maximum temperatures are projected to increase by between 3 and 4.5 °C over much of the savanna, apart from the far southwest where rises of between 4.5 and 6 °C are projected (Fig. 6a). Nearly the whole region (except the far east) is projected to experience maximum temperature rises of between 4.5 and 6 °C under the 90th percentile (Fig. 6c).

Projections of heatwave days spatial variability showed a gradual increase from Mozambique in the east towards Botswana in the west (Fig. 6d-e). The 10th percentile spatial variability projected an increase of 0–2 days over the east, 2–4 days in the central areas and 4–6 in the western (Fig. 6d). Significantly, the 90th percentile projected an increase of 6 to 8 days east of 29°E, with increases of more than 8 heatwave days per annum west of 29°E, toward Botswana.

Projected increases in heatwave days may be associated with rapid rises in maximum temperatures in the far future over the study area (Engelbrecht et al. 2015; Mbokodo et al. 2020) and expansion of arid climate zone (Engelbrecht and Engelbrecht 2016; Jury 2021). Increased frequency of heatwaves may imply persistence and strengthening of the mid-level high pressure systems that prevail over this region, influenced by expansion of the Hadley cell over southern Africa (Engelbrecht et al. 2011; Mahlobo et al. 2019). In addition, rising surface air temperatures may support growth of tress and expansion of Limpopo savanna into patches of grasslands (Engelbrecht and Engelbrecht 2016).

3.2.2 Projected changes in rainfall and minimum relative humidity

The projected changes in far-future rainfall over the Limpopo savanna from an ensemble of six downscalings are shown in Fig. 7a-c, whilst projected changes in minimum relative humidity are shown in Fig. 7d-f. The main changes projected are significant decreases in rainfall and minimum relative humidity, under all three percentiles considered. Greater decreases in rainfall are projected along the escarpment and in the west, towards Botswana, with decreases reaching − 20 mm/month (Fig. 7a-c). Considering that the west of the study region has been shown to be a low rainfall area, such projected changes would cause significant impacts on vegetation. However, as the frequency of extreme rainfall events is also expected to increase, the effect of rainfall decreases on fuel load is not clear.

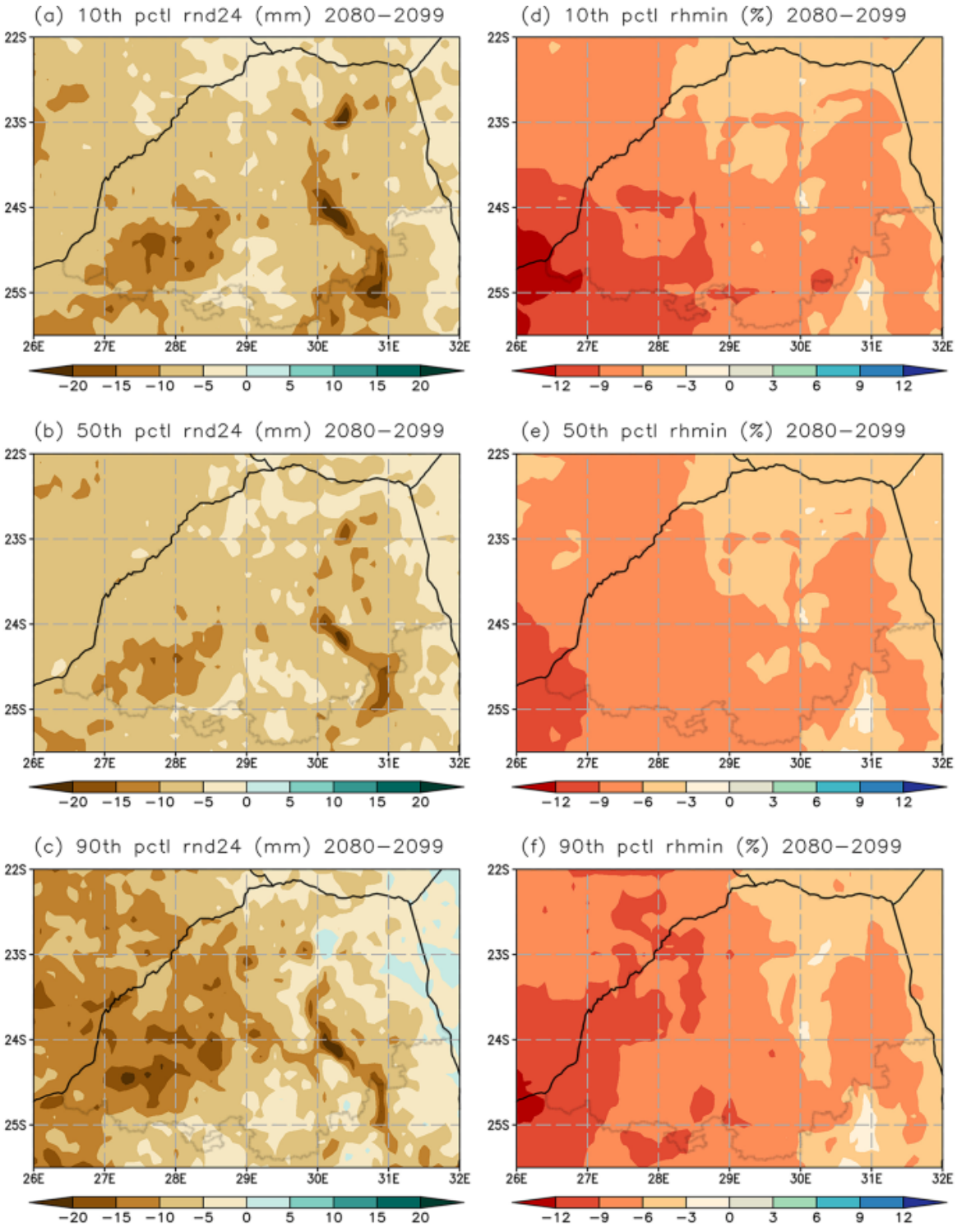

Fig. 7. Far future (2080–2099) projected changes in (a) 10th percentile rainfall (mm/month); (b) 50th percentile rainfall (mm/month); (c) 90th percentile rainfall (mm/month); (d) 10th percentile minimum relative humidity (%); (e) 50th percentile minimum relative humidity (%); and (f) 90th percentile minimum relative humidity (%). Darker shades of brown indicate greater negative anomalies of rainfall whilst darker shades of orange indicate greater negative anomalies of minimum relative humidity

Several other studies have projected drier conditions over the Limpopo savannas under the low mitigation emission scenario (e.g., Engelbrecht et al. 2011; Archer et al. 2018; Engelbrecht and Monteiro 2021). Tropical cyclone tracks are also projected continuously varying northwards to northern Mozambique, hence becoming fewer over North-eastern regions of South Africa, Limpopo province (Malherbe et al. 2013). CORDEX regional climate models have projected decreased rainfall by 0.2 and 0.3 mm /day under 1.5° and 2° global warming levels (Maúre et al. 2018). The spatial extent of projected decreasing rainfall varies with increasing intensity of drought under increasing global warming levels over southern Africa (James and Washington 2013; Maúre et al. 2018). Meteorological droughts are projected increasing consistently in southern Africa in the models under both 1.5 and 2 °C global warming levels (Hoegh-Guldberg et al. 2018). Besides projected decreasing rainfall variabilities, daily rainfall intensities are expected to increase in some regions (Hoegh-Guldberg et al. 2018).

The projected changes in minimum relative humidity (RH) also showed decreasing in the west region of the study area and Botswana (Fig. 7d-f). Most of the study region is projected to experience decreases of minimum relative humidity of between 6 and 9% across all three percentiles (Fig. 7d-f).

3.2.3 Projected changes in wind speeds and soil moisture availability

The projected changes of future of wind speed and soil moisture availability are shown in Fig. 8(a-f). Wind speeds are projected to increase across the northern savanna in the far future under the RCP8.5 emission scenario. The 90th percentile projected higher changes of wind speed particularly in the Limpopo River Basin and the western savanna, and into Botswana (Fig. 8c). Increasing wind speeds may be associated with increasing risk of propagation and spread of forest fires in the far-future under the RCP8.5 emission scenario.

Projections of changes in soil moisture deficiency in the far future period suggest increased deficiencies across the entire study region, under all three percentiles (Fig. 8d-f). Meanwhile, high soil moisture deficiency is associated with severe drought conditions and increasing chance of fire occurrence. Due to the projected increasing change in soil dryness from the 10th, 50th, and 90th percentiles (Fig. 8d-f), the Limpopo savanna should become more vulnerable to extreme drought, wildfire events due to intensified evaporation (Engelbrecht et al. 2015). Projected increasing dry conditions in the Limpopo savanna are influenced by drastic increases in temperatures and projected rainfall deficiency over the study area. In terms of the KBDI 10th percentile, soil moisture deficiency is projected increasing by 50 to 75 mm extending from Botswana and south of the Limpopo savanna (Fig. 8d), hence significantly varying below ~ 24°S and 27°E-31°E (Fig. 8e-f). An increase in soil moisture deficiency by 0–25 mm inches is projected along the boundary between Limpopo savanna, Zimbabwe and Mozambique.

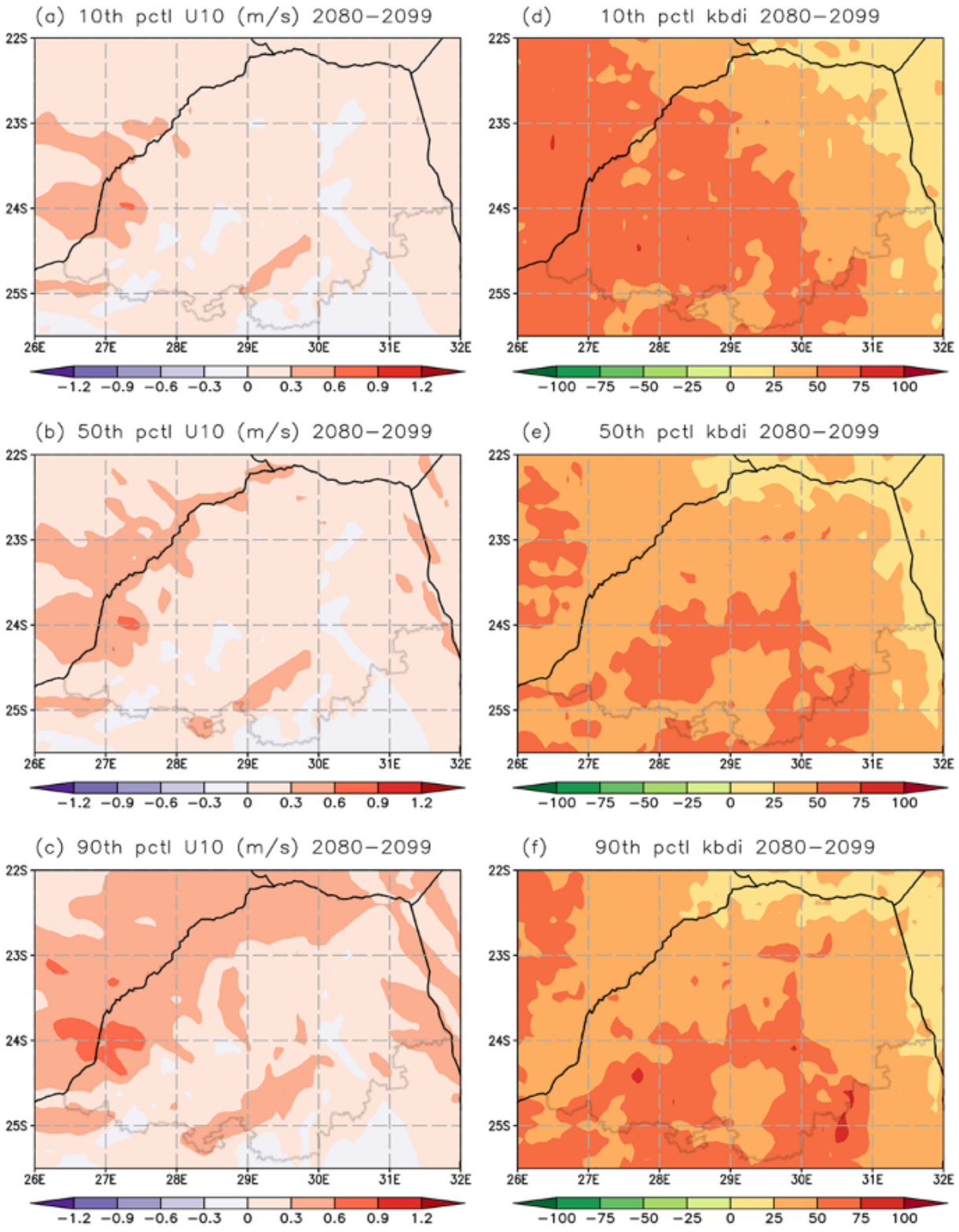

Fig. 8. Far future (2080–2099) projected changes of (a) 10th percentile wind speed (u10) at 10 m (m/s); (b) 50th percentile wind speed at 10 m (m/s); (c) 90th percentile wind speed at 10 m (m/s); (d) 10th percentile kbdi soil moisture deficiency (mm); (e) 50th percentile soil moisture deficiency (mm); and (f) 90th percentile soil moisture deficiency (mm). Darker shades indicate greater positive anomalies on both u10 and kbdi

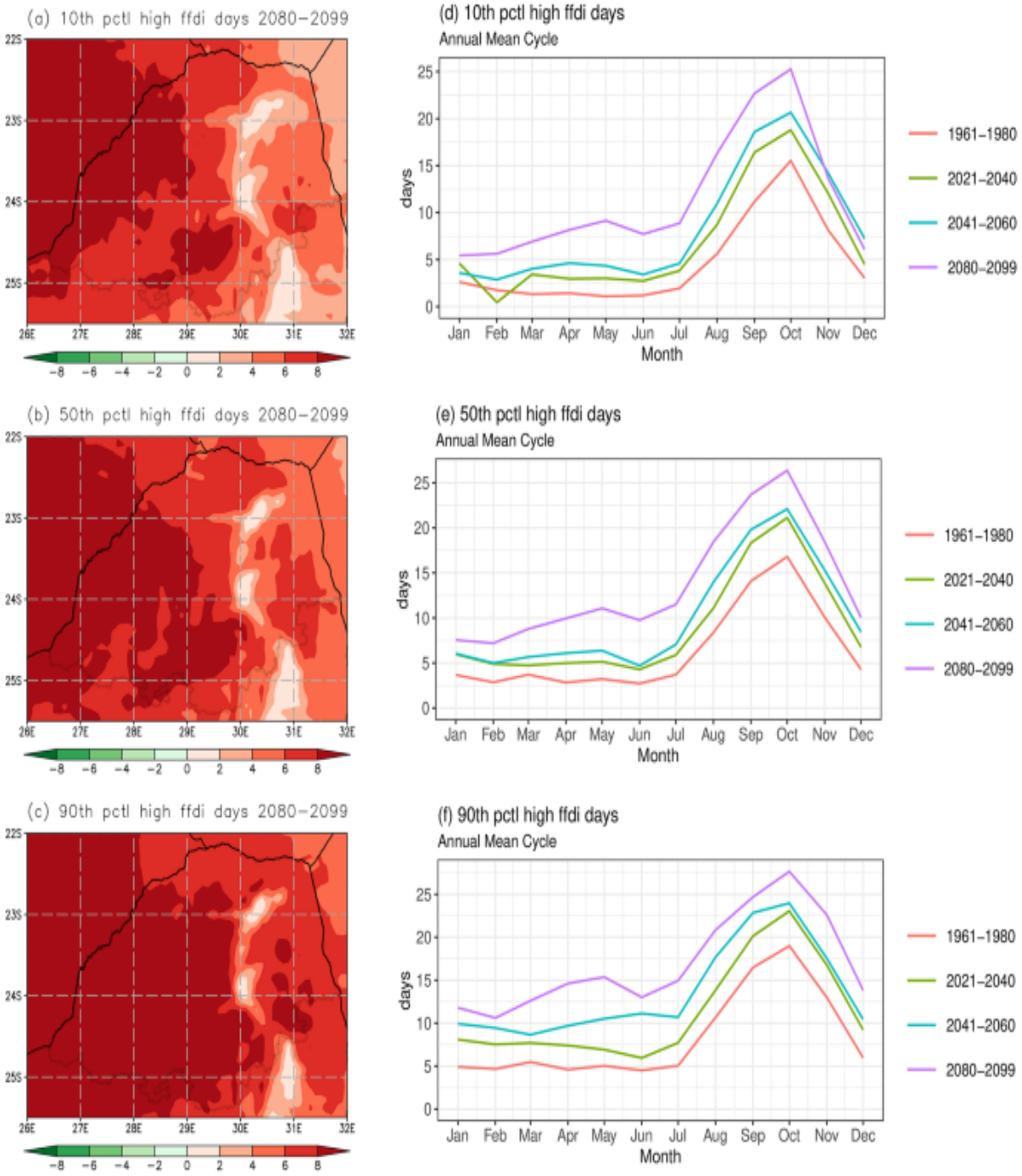

Fig. 9. Far future projected changes in (a) 10th percentile high FFDI days (b) percentile high FFDI days; (c) 90th percentile high FFDI days; (d) 10th percentile mean annual cycle of high FFDI days; (e) 50th percentile mean annual cycle of high FFDI days; and (f) 90th percentile mean annual cycle of high FFDI days. Darker shades of red indicate greater positive anomalies in FFDI days (a-c)

3.2.4 Projected changes in high fire danger days and forest fire risk

Projected changes to high fire danger days over Limpopo savanna during the period 2080–2099 varied significantly with some uncertainties using the 10th, 50th, and 90th percentile

showing more high fire danger days in the western region (Fig. 9a-c). The study found drastic increases in the frequency of high fire danger days across Limpopo savanna, with two days fewer along the Great Escarpment. The western region is projected to undergo extreme changes due to the high fire danger index change by greater than 8 days toward Botswana. Meanwhile, projected changes in high fire danger days over the east and north regions vary within a range of 2–4 days and 4–6 days (Fig. 9b), with the 90th percentile projecting 6–8 days and above (Fig. 9c).

The annual mean cycles of high fire danger days represented in Fig. 8 (d-f) were computed using 10th, 50th and 90th percentile field mean for the spatial coverage (22°S-25.5°S and 26°E-32°E). The reference climate (1961–1980) and three projected futures (2021–2040, 2041–2060 and 2080–2099) showed that the frequency of high fire danger days is relatively low from January to July but begin increasing to the peak in October (Fig. 8d-f). Variations from projected uncertainty showed significant increase in high fire danger days during March-April-May in the far future as shown by the 10th, 50th and 90th percentiles (Fig. 8d-f). Both 10th and 50th percentile showed a peak of 25 days of high fire danger index during period 2080–2099. The 90th percentile projection showed a peak of more than 25 days in October (Fig. 8f). High fire danger days are projected to have increased by an average of 10 days during the peak in October (Fig. 8d-f). The study by Engelbrecht et al. (2015) also made a similar projection, suggesting that projected high fire danger days may lead to occurrence of catastrophic wildfire events in future. Since rising temperatures favour growth of woody vegetation, frequent occurrence of wildfire may reserve tree-C4 grasses interaction over the Limpopo savanna (Engelbrecht and Engelbrecht 2016). Projections of decreasing minimum relative humidity suggest increasing forest fire risk in the far- future over the study area. Mean annual cycles of high fire danger days in the future showed a peak in October, similar to the peaks in number of fires observed in September and October during fire season over Limpopo savanna by Strydom and Savage (2016). A secondary autumnal (March-May) peak becomes distinct in the far future, perhaps associated with a shorter rainy season.

4 Summary and conclusions

Wildfires pose a significant risk to livelihoods, human health and wellbeing, air quality, ecosystems and agricultural activities. Whilst global warming and climate change may be compounding wildfire activity, fire emissions also feedback on the climate. Thus, the study of fire risk over an area that is prone to fire is very important under increasing global warming levels due to climate change. In this study, we presented future climate change projections for the far future period (2080–2099) over South Africa's Limpopo savanna under the worst case RCP8.5 emission scenario. An ensemble of six CMIP5 GCMs dynamically downscaled though RCM CCAM to a high resolution of 8 km were employed. The purpose of using an ensemble of six CMIP5 for future projections is due to their ability to simulate realistic reference climatologies whilst also providing confidence in the future projections and associated uncertainties. However, whilst the number of ensemble members is important, the choice of models may even be more critical as some models are considered 'hot' (Hausfather et al. 2022) and unrealistic. The assumption that all models contribute equally to the skill of the ensemble may also be misleading. During the evaluation of the CMIP climate sensitivity for IPCC in 2019, climate models with higher sensitivities in relation to greenhouse warming were considered too hot (Voosen 2022). The six members of the ensembles analysed in the study showed high skills are therefore not considered hot.

The models employed here were verified using a Taylor diagram and compared with ERA5-Land observations of the reference climate (1961–1980). Model verification increases confidence in using climate models for realistic presentation of future climate change variabilities. Verification revealed that models simulate unprecedented increases in surface air temperatures over the Limpopo savanna. An analysis of the observed ERA5-land 2 m air temperature trend showed an average increase from 0.3 °C to > 1° C on the savanna during the period 1961 to 2020. The warming trends are consistent with several studies such as Engelbrecht et al. (2015), Jury (2018), Kruger and Shongwe (2004) and others. The rising trend in temperatures was projected to persist with increases of between 4.5 and 6 °C during the far future period 2080–2099 over the Limpopo savanna. The study projected a drier and warmer climate over the Limpopo savanna consistent with the recent literature. Changes in the far future projections showed significant uncertainty in deficiency of water balance metrics including rainfall, soil moisture availability and relative humidity.

The risk of high fire danger days was projected increasing over Limpopo savanna under the RCP8.5 (business as usual) scenario. Models' results agree with future projections from other studies focusing on the increasing temperatures and an elongated future drying. We found that the number of high fire danger days is projected to increase to about 25 days in the far future under the worst-case scenario. The risk of wildfire activity seems to also become significant during the austral autumn, suggesting an early cessation to the summer rains in future. A recent UN report (United Nations Environment Programme 2022) projects more frequent wildfires occurring in several regions of the world, including the savannas. The report also highlights impacts of wildfires on the carbon cycle, human health, economies, wildlife and water catchments.

This study contributes new knowledge to the understanding of forest fire risk on the savannas, via an ensemble of very high-resolution climate models at the regional scale. Forest fire risk is changing in response to recent unprecedented temperature increases coupled with repeated heat waves, which appear to be modulating fire intensity on the African savanna. It is important to emphasize that future fire risk is a function of several variables other than the climate (United Nations Environment Programme 2022). Measures to mitigate and manage forest fire risk are critical towards natural disaster risk reduction in future.

Acknowledgements

This study was supported by generous funding from South Africa's National Research Foundation (NRF). We acknowledge the anonymous reviewers whose comments helped us improve the manuscript considerably.

Funding

This study was supported and funded by the South Africa's National Research Foundation (NRF).

Contributions

M.V.S. conceptualization, analyses, writing the original manuscript, H.C supervision, revised and edited the manuscript, F.A.E conceptualization, supervision, model simulations and comments, M.M.B edited manuscript and suggested changes, T.N edited the manuscript and

provided comments, T.P.M edited the manuscript and provided comments, I.L.M edited the manuscript and provided comments, and F.M.M supervision and provided comments.

Data Availability

The CMIP5 GCM models were obtained from the Copernicus Climate Data Store website https://cds.climate.copernicus.eu/#!/home.

References

Archer ER, Engelbrecht FA, Hänsler A, Landman W, Tadross M, and Helmschrot J (2018) Seasonal prediction and regional climate projections for southern Africa. Biodiv Ecol 6:14–21. https://doi.org/10.7809/b-e.00296

Archibald S (2016) Managing human component of fire regimes: lessons from Africa. Philosoph Transac Royal Society B Biol Sci 371(1696):20150346

Bajocco S, Ferrara C, Guglietta D, Ricotta C (2019) Fifteen years of changes in fire ignition frequency in Sardinia (Italy): a rich-get-richer process. Ecol Ind 104:543–548

Barimalala R, Blamey RC, Desboiolles F, Reason CJC (2021) The influence of southeastern african river valley jets on regional rainfall. Clim Dyn. https://doi.org/10.1007/s00382-021-05846-1

Berry RS, Kulmatiski A (2017) Savanna response to precipitation intensity. PLoS ONE 12(4):e01754402. https://doi.org/10.1371/journal.pone.0175402

Bi D, Dix M, Marsland SJ, O'Farrell S, Rashid H, Uotila P, Hirst AC, Kowalczyk E, Golebiewski M, Sullivan A, Yan H (2013) The ACCESS coupled model: description, control climate and evaluation. Australian Meteorol Oceanogr J 63(1):41–64

Bornmann L, Leydesdorff L, Mutz R (2013) The use of percentiles and percentile rank classes in the analysis of bibliometric data: Opportunities and limits. J informetrics 7(1):158–165

Bowman DM, Kolden CA, Abatzoglou JT, Johnston FH, van der Werf GR, Flannigan M (2020) Vegetation fires in the Anthropocene. Nat Reviews Earth Environ 1(10):500–515

Chikoore H, Bopape MM, Ndarana T, Muofhe TP, Gijben M, Munyai RB, Manyanya TC, Maisha R (2021) Synoptic structure of a sub-daily extreme precipitation and flood event in Thohoyandou, northeastern South Africa. Weather and Climate Extremes 33:10327. https://doi.org/10.1016/j.wace.2021.100327

Chikoore H, Jury MR (2021) South african drought, deconstructed. Weather and Climate Extremes 33:100334. https://doi.org/10.1016/j.wace.2021.100334

Cochrane MA, Bowman DM (2021) Manage fire regimes, not fires. Nat Geosci 14(7):455–457

Countryman CM (1972) The Fire Environment Concept. USDA Forest Service, Pacific Southwest Forest and Range Experiment Station, Berkeley, p 12

Crutzen PJ, Heidt LE, Krasnec JP, Pollock WH, Seiler W (1979) Biomass burning as a source of atmospheric gases CO, H2, N2O, NO, CH3Cl and COS. Nature 282:253–256. https://doi.org/10.1038/282253a0

de Groot RS, Alkemade R, Braat L, Hein L, Willemen L (2010) Challenges in integrating the concept of ecosystem services and values in landscape planning, management and decision making. Ecol Complex 7(3):260–272

Dowdy AJ (2018) Climatological variability of Fire Weather in Australia. J Appl Meteorol Climatology. https://doi.org/10.1175/JAMC-D-17-0167.1

Driver P, Reason CJC (2017) Variability in the Botswana High and its relationship with rainfall and temperature characteristics over southern Africa. Int J Climatol 37(1):570–581

Duane A, Brotons L (2018) Synoptic weather conditions and changing fire regimes in a Mediterranean environment. Agric For Meteorol 253:190–202 ISSN 0168–1923. https://doi.org/10.1016/j.agrformet.2018.02.014

Dunne JP, Horowitz LW, Adcroft AJ, Ginoux P, Held IM, John JG, Krasting JP, Malyshev S, Naik V, Paulot F, Shevliakova E (2020) The GFDL Earth System Model version 4.1 (GFDL-ESM 4.1): Overall coupled model description and simulation characteristics. J Advn Model Earth Syst 12(11):e2019MS002015

Dyson LL, van Heerden J (2002) A model for the identification of tropical weather systems over South Africa. Water SA 28(3):ISSN0378–4738

Engelbrecht CJ, Engelbrecht FA (2016) Shifts in Köppen-Geiger climate zones over southern Africa in relation to key global temperature goals. Theoret Appl Climatol 123:247–261. https://doi.org/10.1007/s00704-014-1354-1

Engelbrecht F, Adegoke J, Bopape MJ, Naidoo M, Garland R, Thatcher M, McGregor J, Katzfey J, Werner M, Ichoku C, Gatebe C (2015) Projections of rapidly rising surface temperatures over Africa under low mitigation. Environ Res Lett 10(8):085004

Engelbrecht FA, Landman WA, Engelbrecht CJ, Landman S, Bopape MM, Roux B, McGregor JL, Thatcher M (2011) Multi-scale climate modelling over Southern Africa using a variable-resolution global model. Water SA 37(5):647–658

Engelbrecht F, Monteiro P (2021) Climate Change: the IPCC's latest assessment report. Quest 17(3):34–35

Flannigan MD, Krawchuk MA, de Groot WJ, Wotton BM, Gowman LM (2009) Implications of changing climate for global wildland fire. Int J Wildland Fire 18:483–507

Gannon CS, Steinberg NC (2021) A global assessment of wildfire potential under climate change utilizing Keetch-Byram drought index and land cover classifications. Environmental Research Communications, 3(3), p.035002

Gent PR, Yeager SG, Neale RB, Levis S, and Bailey DA (2010) Improvements in a half degree atmosphere/land version of the CCSM. Clim Dynm 34(6):819–833

Gordijn PJ, Everson TM, O'Connor TG (2018) Resistance of Drakensberg grasslands to compositional change depends on the influence of fire-return interval and grassland structure on richness and spatial turnover. *Perspectives in Plant Ecology*. Evol Syst 34:26–36

Harrison MSJ (1984) A generalised classification of south african rain-bearing synoptic systems. J Climatol 4:547–560

Hart NCG, Reason CJC, Fauchereau N (2010) Tropical–extratropical interactions over southern Africa: three cases of heavy summer season rainfall. Mon Weather Rev 138(7):2608–2623

Hart NCG, Reason CJC, Fauchereau N (2013) Cloud bands over southern Africa: seasonality, contribution to rainfall variability and modulation by the MJO. Clim Dyn 41:1199–1212

Hausfather Z, Marvel K, Schmidt GA, Nielsen-Gammon JW, Zelinka M (2022) Climate simulations: Recognize the 'hot model'problem. *Nature 605:26–29*

Hoegh-Guldberg O, Jacob D, Bindi M, Brown S, Camilloni I, Diedhiou A, Djalante R, Ebi K, Engelbrecht F, Guiot J, Hijioka Y (2018) Impacts of 1.5 C global warming on natural and human systems. Global warming of 1.5 C. An IPCC special report

Hoffmann WA, Schroeder W, Jackson RB (2002) Positive feedbacks of fire, climate and vegetation and the conversion of tropical savanna. Geophys Res Lett 29:22. https://doi.org/10.1029/2002GL01524

Hovenden MJ, Leuzinger S, Newton PC, Fletcher A, Fatichi S, Lüscher A, Reich PB, Andresen LC, Beier C, Blumenthal DM, Chiariello NR (2019) Globally consistent influences of seasonal precipitation limit grassland biomass response to elevated CO2. Nat plants 5(2):167–173

Hu Z, Chen X, Zhou Q, Chen D, Li J (2019) DISO: a rethink of Taylor diagram. Int J Climatol 39(5):2825–2832

James R and Washington R (2013) Changes in African temperature and precipitation associated with degrees of global warming. Clim Change 117:59–872

Jury MR (2018) Climate trends across South Africa since 1980. Water SA 44(2):297–307

Jury MR (2021) Spreading of the semi-arid climate across South Africa. J Water Clim Change 12(8):3734–3749. https://doi.org/10.2166/wcc.2021.187

Kasischke ES and Hoy EE (2012) Controls on carbon consumption during Alaskan wildland fires. Global Change Biol 18:685–699.

Keeley JE, Alexandra D, and Syphard AD (2016). Climate change and future fire regimes: examples from California. Geosciences 6:37. https://doi.org/10.3390/geosciences6030037

Keeley JE, Syphard AD (2021) Large California wildfires: 2020 fires in historical context. Fire Ecol 17(1):1–11

Keetch JJ, Byram GM (1968) A drought index for forest fire control, vol 38. US Department of Agriculture, Forest Service, Southeastern Forest Experiment Station, pp 1–32

Kraaij T, Baard JA, Arndt J, Vhengani L, Van Wilgen BW (2018) An assessment of climate, weather, and fuel factors influencing a large, destructive wildfire in the Knysna region, South Africa. Fire Ecol 14(2):1–12

Kruger A, Shongwe S (2004) Temperature trends in South Africa: 1960–2003. Int J Climatol 15:1929–1945

Laris P, Jacobs R, Kone M, Dembele F, Rodrigue MC (2020) Determinants of fire intensity in working landscapes of an african savanna. Fire Ecol 16:27. https://doi.org/10.1186/s42408-020-00085-xLobo AK, Catarino IC, Silva EA, Centeno DC, Domingues DS (2022) Physiological and molecular responses of woody plants exposed to future atmospheric CO2 levels under abiotic stresses. Plants 11(14):1880

Lyon B (2009) Southern Africa summer drought and heat waves: observations and coupled model behavior. J Clim 22(22):6033–6046

Mahlobo DD, Ndarana T, Grab S, Engelbrecht F (2019) Integrated climatology and trends in the subtropical Hadley cell, sunshine duration and cloud cover over South Africa. Int J Climatol 39(4):1805–1821

Malherbe J, Engelbrecht FA, Landman WA (2013) Projected changes in tropical cyclone climatology and landfall in the Southwest Indian Ocean region under enhanced anthropogenic forcing. Clim Dyn 40(11):2867–2886

Maponya P, Madakadze C, Mbili N, Dube ZP, Nkuna T, Makhwedzhana M, Tahulela T, Mongwaketsi K (2021) Potential constraint of rainfall availability on the establishment and expansion of agroforestry in the Mopani District, Limpopo Province in South Africa. AGROFOR Int J 6:1

Maúre G, Pinto I, Ndebele-Murisa M, Muthige M, Lennard C, Nikulin G, Dosio A, Meque A (2018) The southern african climate under 1.5 C and 2 C of global warming as simulated by CORDEX regional climate models. Environ Res Lett 13(6):065002

Martens C, Hickler T, Davis-Reddy C, Engelbrecht F, Higgins SI, von Maltitz GP, Midgley GF, Pfeiffer M, Scheiter S (2020) Large uncertainties in future biome changes in Africa call for flexible climate adaptation strategies. Glob Change Biol 27:340–358. https://doi.org/10.1111/gcb.15390

Mbokodo I, Bopape MJ, Chikoore H, Engelbrecht F, Nethengwe N (2020) Heatwaves in the future warmer climate of South Africa. Atmosphere 11(7):712

McGregor JL (2005) CCAM: geometric aspects and dynamical formulation. CSIRO Atmospheric Research Technical Paper No 70:43

Müller WA, Jungclaus JH, Mauritsen T, Baehr J, Bittner M, Budich R, Bunzel F, Esch M, Ghosh R, Haak H, Ilyina T (2018) A higher-resolution version of the max planck institute earth system model (MPI-ESM1. 2-HR). J Adv Model Earth Syst 10(7):1383–1413

Moshobane MC, Olowoyo JO, Middleton L (2021) Alien plant species of Haenertsburg Village, Limpopo Province, South Africa

Munday C, Washington R, Hart N (2021) African low-level jets and their importance for water vapor transport and rainfall.Geophysical Research Letters, 48(1), e2020GL090999.

Muñoz Sabator J (2021) ERA5-Land monthly averaged data from 1950 to 1980. Copernicus Climate Change Servives (C3S) Climate Data Store (CDS). https://cds.climate.copernicus.eu/cdsapp#!/search?type=dataset. Accessed 31 March 2022)

NASA (2022) Global Temperature. https://climate.nasa.gov/vital-signs/global-temperature/. Accessed 17 May 2022

Ndarana T, Rammopo TS, Reason CJC, Bopape M, Engelbrecht F, Chikoore H (2022) Two types of ridging South Atlantic Ocean anticyclones over South Africa and the associated dynamical processes. Atmos Res 265:105897. https://doi.org/10.1016/j.atmosres.2021.105897

Nembilwi N, Chikoore H, Kori E, Munyai RB, Manyanya TC (2021) The occurrence of Drought in Mopani District Municipality, South Africa: impacts, vulnerability and adaptation. Climate 9(4):61

NIDIS (2022) Keetch-Byram Drought Index (KBDI) – U.S. Forest Service. https://www.drought.gov/data-maps-tools/keetch-byram-drought-index. Accessed 16 May 2022.

Noble I R, Bary GAV, Gill AM (1980) McArthur's fire-danger meters expressed as equations Aust. Journal of Ecology, 5 201–3

Piñol J, Terradas J, Lloret F (1998) Climate warming, wildfire hazard and wildfire occurrence in coastal eastern Spain. Clim Change 38:345–357

Platt WJ, Orzell SL, Slocum MG (2015) Seasonality of Fire Weather strongly Influences Fire Regimes in South Florida Savanna-Grassland Landscapes. PLoS ONE 10(1):e0116952. https://doi.org/10.1371/journal.pone.0116952

Rapolaki RS, Blamey RC, Hermes JC, Reason CJC (2020) Moisture sources associated with heavy rainfall over the Limpopo River Basin, southern Africa. Clim Dyn 55(5):1473–1487

Roces-Díaz JV, Vayreda J, De Cáceres M, García-Valdés R, Banqué-Casanovas M, Morán-Ordóñez A, Brotons L, de-Miguel S, Martínez-Vilalta J (2021) Temporal changes in Mediterranean forest ecosystem services are driven by stand development, rather than by climate-related disturbances. For Ecol Manag 480:118623

Rogers BM, Balch JK, Goetz SJ, Lehmann CE, Turetsky M (2020) Focus on changing fire regimes: interactions with climate, ecosystems, and society. Environ Res Lett 15(3):030201

Sankaram M (2019) Drought and ecological future of tropical savanna vegetation. J Ecol 10(4):1531–1549

Schmidt IB, Eloy L (2020) Fire regime in the brazilian Savanna: recent changes, policy and management. Flora 268:151613

Seland Ø, Bentsen M, Olivié D, Toniazzo T, Gjermundsen A, Graff LS, Debernard JB, Gupta AK, He YC, Kirkevåg A, Schwinger J (2020) Overview of the norwegian Earth System Model (NorESM2) and key climate response of CMIP6 DECK, historical, and scenario simulations. Geosci Model Dev 13(12):6165–6200

Spavins-Hicks ZD, Washington R, Munday C (2021) The Limpopo Low-Level Jet: Mean Climatology and Role in Water Vapor Transport. J Geophys Research: Atmos 126(16):e2020JD034364

Strydom S, Savage MJ (2016) A spatio-temporal analysis of fires in South Africa. South Afr J Sci 112(11–12):1–8

Taylor KE (2001) Summarizing multiple aspects of model performance in a single diagram. J Geophys Research: Atmos 106(D7):7183–7192

Taylor KE (2005) Taylor diagram primer.Work. Pap,1–4

Thatcher M, McGregor J, Dix M, Katzfey J (2015) A new approach for coupled regional climate modeling using more than 10,000 cores. *International Symposium on Environmental Software Systems* 599–607

Thevakaran A, McGregor JL, Katzfey J, Hoffmann P, Suppiah R, Sonnadara DUJ (2015) An assessment of CSIRO Conformal Cubic Atmospheric Model simulations over Sri Lanka. Clim Dyn 46:1861–1875. https://doi.org/10.1007/s00382-015-2680-4

Tyson PD, Preston-Whyte RA (2000) Weather and climate of southern Africa. Oxford University Press, South Africa

United Nations Environment Programme (2022) Spreading like wildfire – the rising threat of extraordinary Landscape fires. A UNEP Rapid Response Assessment. Nairobi

Usman MT, Reason CJC (2004) Dry spell frequencies and their variability over southern Africa. Climate Res 26(3):199–211

Val A, de la Peña P, Duval M, Bansal S, Colino F, Culey J, Hodgskiss T, Morrissey P, Murray A, Murungi M, Neumann FH (2021) The place beyond the trees: renewed excavations of the Middle Stone Age deposits at Olieboomspoort in the Waterberg Mountains of the south african Savanna Biome. Archaeol Anthropol Sci 13(7):1–32

Van der Walt AJ, Fitchett JM (2020) Statistical classification of south african seasonal divisions on the basis of daily temperature data. South Afr J Sci 116(9–10):1–15. https://doi.org/10.17159/sajs.2020/7614

Viedma O, Urbieta IR, Moreno JM (2018) Wildfires and the role of their drivers are changing over time in a large rural area of west-central Spain. Sci Rep 8(1):1–13. https://doi.org/10.1038/s41598-018-36134-4

Voldoire A, Sanchez-Gomez E, Salas y Mélia D, Decharme B, Cassou C, Sénési S, Valcke S, Beau I, Alias A, Chevallier M, Déqué M (2013) The CNRM-CM5. 1 global climate model: description and basic evaluation. Clim Dyn 40(9):2091–2121

Voosen P (2022) 'Hot'climate models exaggerate Earth impacts. Sci (New York NY) 376(6594):685–685

Wainwright CM, Black E, Allan RP (2021) Future changes in wet and dry season characteristics in CMIP5 and CMP6 simulations. J Hydrometeology 22(9):2339–2357

Yadav I, Devi N 2(019) Biomass burning, regional air quality, and climate change. *Encyclopedia of Environmental Health*, 386 – 39. https://doi.org/10.1016/B978-0-12-409548-9.11022-X